Contents lists available at SciVerse ScienceDirect

# Atmospheric Research

# Study of the urban heat island in a coastal Mediterranean City: The case study of Thessaloniki, Greece

Theodore M. Giannaros *, Dimitrios Melas

*Laboratory of Atmospheric Physics, Aristotle University of Thessaloniki, PO BOX 149, 54124, Thessaloniki, Greece*

## ARTICLE INFO

## ABSTRACT

The urban heat island in the coastal city of Thessaloniki, Greece, is investigated using near-surface temperature data measured at 7 sites in the greater Thessaloniki area for the 1-year period from March 2008 to February 2009. The urban heat island in Thessaloniki is stronger in the nighttime than in the daytime and decreases with increasing wind speed, while there are indications that it is more pronounced during the warm half of the year. Observations of the maximum urban heat island intensity range from 2 °C to 4 °C and from 1 °C to 3 °C during the warm and the cold part of the year, respectively, showing a smaller variability during the summer moths than in the winter. Greatest values are more usually observed following sunset, whereas minimum values are detected during solar peak hours. A regression analysis is carried out to investigate the impact of moisture availability and wind speed on the development of the urban heat island in Thessaloniki. It is found that the nocturnal heat island results to increased nighttime water vapor pressure in the urban areas, whereas during the day the heat island intensity and urban/semi-rural water vapor pressure differences are found to be anti-correlated. Furthermore, the intensity of Thessaloniki's heat island appears to decrease significantly when wind speed exceeds 4 m/s. The impact of the urban heat island on human thermal comfort in Thessaloniki is also investigated, computing hourly values of the discomfort index and the approximated wet bulb globe temperature. The center of the city is found to exhibit the highest discomfort index and approximated wet bulb globe temperature values. In addition, the urban heat island is found to have a negative impact on thermal comfort on most of the observed occasions. In particular, a 1.5 °C increase in the urban heat island intensity appears to result to an average 1 °C increase in discomfort index and 1.4 °C increase in approximated wet bulb globe temperature of the urban area on about 50% and 75% of the cases, respectively.

## 1. Introduction

Urbanization induces significant atmospheric and surface modifications, leading to a modified thermal climate that is generally warmer than the surrounding non-urbanized areas. This phenomenon is well known as the urban heat island (UHI). Unless otherwise indicated, it describes the excess warmth of the urban atmosphere compared to the rural surroundings (Voogt and Oke, 2003). According to Oke (1982), heat islands can be observed in either the urban canopy layer (UCL), extending from the ground up to the mean roof level, or the urban boundary layer (UBL). This phenomenon was first documented by Howard (1883) and has since been studied in many cities around the world. Throughout the last decade, heat islands have been observed and examined in cities as diverse as Lódz, Poland (Klyzik and Fortuniak, 1999), Athens, Greece (Livada et al., 2002), Beijing, China (Miao et al., 2009) and Aveiro, Portugal (Pinho and Orgaz, 2000). A summary of the UHI studies carried out in Europe during the last 15 years can be found in Santamouris (2007).

* Corresponding author. Tel.: +30 2310998183; fax: +30 2310 998090.
*E-mail address:* thgian@auth.gr (T.M. Giannaros).

There are numerous reasons to study the UHI effect as it involves social, economic and environmental issues. Today, nearly half of the world's population is affected by UHIs and this number will only increase as the urban population is expected to reach 5 billion by year 2030 (World Urbanization Prospects, 2007). Many of the fast growing urban areas reside in developing countries, where the lack of urban planning and heat island mitigation strategies only compound the problem.

Overheating in urban areas could be significantly exacerbated as a result of the UHI effect. During heat waves, death rates in cities are often much higher than in the rural surroundings (e.g. Buechley et al., 1972; Clarke, 1972; Jones et al., 1982; Smoyer, 1998). According to epidemiologic studies, people living in urban areas experience an elevated risk death compared to those living in suburban or rural areas, as a result of the increased temperatures (Conti et al., 2005; Matzarakis et al., 2009). However, the wider picture should be also considered. While heat islands could result to increased summertime heat-related mortality, they could also lead to fewer cold-related deaths during winter (Mavrogianni et al., 2011). According to Hacker et al. (2005), the rise in urban temperatures has a positive impact on thermal comfort during winter.

The increased air temperature in urban areas can also accelerate certain atmospheric chemical cycles, leading to an increase in ground-level ozone concentrations (Rosenfeld et al., 1998). The deterioration of air quality leads to more incidences of respiratory illnesses, another adverse impact of the UHI effect on public health.

Last but not least, UHIs have proven to cause a significant increase in energy demand for cooling purposes (Konopacki and Akbari, 2002), which can, in turn, lead to significant financial losses. For instance, Konopacki and Akbari (2002) estimated that the city of Houston, United States, alone could save up to $82 M on the annual basis by implementing heat island mitigation strategies. Santamouris et al. (2001) found that the cooling load of urban buildings in Athens may be doubled and the peak electricity load for cooling purposes may be tripled, as a result of the elevated temperatures due to the UHI.

Heat islands develop as a result of the urban/rural energy budget differences (Oke, 1982). In terms of the radiation balance, the differences between urban and rural areas are considered to be small (Oke, 1982; Arnfield, 2003). The larger daytime energy input of urban areas due to the lower albedo is mostly compensated by the larger nighttime radiative loss due to the higher emissivity (Christen and Vogt, 2004). However, there are interesting exceptions to this generalization. For instance, Grimmond et al. (1996) measured 19% more net all-wave radiation for a Los Angeles, United States, suburb with 30% vegetation cover than for an adjacent neighborhood with 10% cover. The role of vegetation becomes even more important when considering the partitioning of the available radiant energy. Typically, vegetation covers only a small fraction of the surface in cities. Consequently, evapotranspiration is significantly reduced and urban areas partition, almost exclusively, their radiant energy into sensible rather than latent heat (Oke, 1982). The presence of water surfaces in urban areas also plays an important role, generally reducing air temperature (e.g. Chang et al., 2007). The modification of the urban

energy balance due to the lower albedo and the reduced evapotranspiration results to a higher urban energy input during daytime, as demonstrated in the study of Christen and Vogt (2004). This excess energy is usually converted into storage, as the thermal properties of urban materials (e.g. heat capacity, thermal conductivity) and the complex, three-dimensional urban geometry significantly increase the storage heat flux in urban areas (e.g. Grimmond and Oke, 1995, 1999). Urban surfaces begin to release the stored energy during the evening transition (Christen and Vogt, 2004), slowing down the cooling rate of urban areas and generating the urban/rural temperature contrast (i.e. the UHI). The design values of the sky view factor also play an important role in maintaining the UHI throughout the night by limiting the net longwave radiation loss of urban areas (Arnfield, 2003; Giridharan et al., 2004). Last but not least, UHI development can be significantly influenced by anthropogenic heat flux. In general, a higher release of anthropogenic heat could result to a more intense UHI, especially in early morning and late afternoon hours when the energy balance is not dominated by the incoming solar radiation (Memon et al., 2009).

There are many factors that influence the temperature difference between the urban and rural areas, also called the UHI intensity (UHII). Most UHI studies agree that the heat island experienced by many cities is stronger during nighttime hours and less pronounced in daytime. Jauregui (1997) reported that 75% of the total observations for positive UHII (i.e. higher temperatures in urban areas) were recorded during the night, whereas only 25% were evident in daytime hours. Montavez et al. (2000) also showed that the highest UHII values are observed overnight and the least during the day, while Kim and Baik (2002) reported that the nighttime UHII values were about 3.3 times larger than in the daytime.

UHII has also been reported to be affected by temporary effect variables in certain ways. Pongracz et al. (2006) reported that anticyclone conditions increase UHII, whereas under cyclonic conditions UHII values appear to decrease (e.g. Kassomenos and Katsoulis, 2006). Furthermore, many studies have showed that the UHII is negatively correlated with wind speed and cloud cover (e.g. Kim and Baik, 2005; Oke, 1982; Papanikolaou et al., 2008). Conversely, several studies have reported that the UHI effect is positively correlated with either the city population (e.g. Hung et al., 2006; Kim and Baik, 2004) or the population density (e.g. Coutts et al., 2003; Steeneveld et al., 2011; Streutker, 2003).

Arnfield (2003) summarizes the influence of various factors on the UHII as follows: UHII decreases with increasing wind speed; UHII decreases with increasing cloud cover; UHII is stronger during the summer or the warm part of the year; UHII tends to increase with increasing city size and population; and UHII is higher during nighttime hours than during the day.

Research into the UHI effect requires detailed and extensive air temperature measurements. These measurements can be helpful for determining the UHII, which is calculated as the spatially averaged air temperature difference between an urban and the surrounding suburban/rural area(s) (Kim and Baik, 2005). The field measurement approach was first used by Howard in 1818 to study the UHI of the city of London, Great Britain. In the meantime, many UHI observational studies have been conducted in different cities around

the world. Results have been mostly used to determine the spatial distribution and the intensity of the UHI effect within a city. A summary of such UHI studies can be found in Arnfield (2003). Santamouris (2007) also provided a comprehensive review of observational UHI studies, in particular for European cities.

Regarding Greece, the number of observational UHI studies is considered to be rather restricted, while most of them focus on the capital of Athens. As early as in 1987, Katsoulis (1987) conducted a climatological study of air temperature in Athens, Greece, concluding that urbanization may be responsible for the increase of minimum temperatures. Katsoulis and Theoharatos (1995) analyzed a 22-year air temperature dataset to provide indications of the UHI in Athens. Philandras et al. (1999) examined the mean monthly maximum and minimum temperature records of an urban and a rural site in Athens to study the effect of urbanization. Livada et al. (2002) used observations from 20 air temperature measurement stations for determining places in the greater Athens area where the heat island effect is more pronounced. The meso-scale and macro-scale aspects of the UHI in Athens were examined in the study of Kassomenos and Katsoulis (2006). More recently, Kolokotsa et al. (2009) provided an observational study of the UHI in the coastal city of Hania, Greece, while Giannopoulou et al. (2011) presented a comprehensive study of the characteristics of the summer UHI in Athens.

To date, the UHI in Thessaloniki, Greece, has received rather little attention from the scientific community. There are only a few studies on this subject, including the previous works of Giannaros et al. (2010), Poupkou et al. (2011) and Kantzioura et al. (2012). To fill this knowledge gap, the current paper aims to describe the spatial and temporal characteristics of the UHI by analyzing a 1-year dataset of hourly air temperature and humidity measurements carried out at 6 urban sites and 1 semi-rural site in the greater area of Thessaloniki. The influence of moisture availability and wind speed on the intensity of the heat island is also investigated. In particular, the current study examines the interconnection between the UHI and the so-called urban moisture excess (UME) phenomenon, which has never been accounted for in previous heat island studies focusing on Greek cities. Furthermore, the intensity of the UHI is linked to human thermal comfort by computing the well-known discomfort index and the approximated wet bulb globe temperature.

Thessaloniki is the second largest city of Greece as regards the number of inhabitants (ca 800,000). The city is situated in Northern Greece and is built-up along the North-East coast of the Thermaikos gulf. The Hortiatis mountain, 1200 m high, dominates to the east of the city, whereas the western side of it is an extended flat area where the industrial zone of Sindos is located. The city is strongly influenced by the sea to the south (Fig. 1). The climate of Thessaloniki can be described as Mediterranean with generally hot and dry summers, and mild and wet winters. The annual mean temperature is 15.9 °C, the annual mean relative humidity is 62.4%, the annual mean precipitation is 448.7 mm, the annual mean wind speed is 5.6 m/s, and the prevailing wind direction is north-west [Climatological values averaged from 1959 to 1997 (Hellenic National Meteorological Service)]. In addition, the city is exposed to frequent sea breezes throughout the
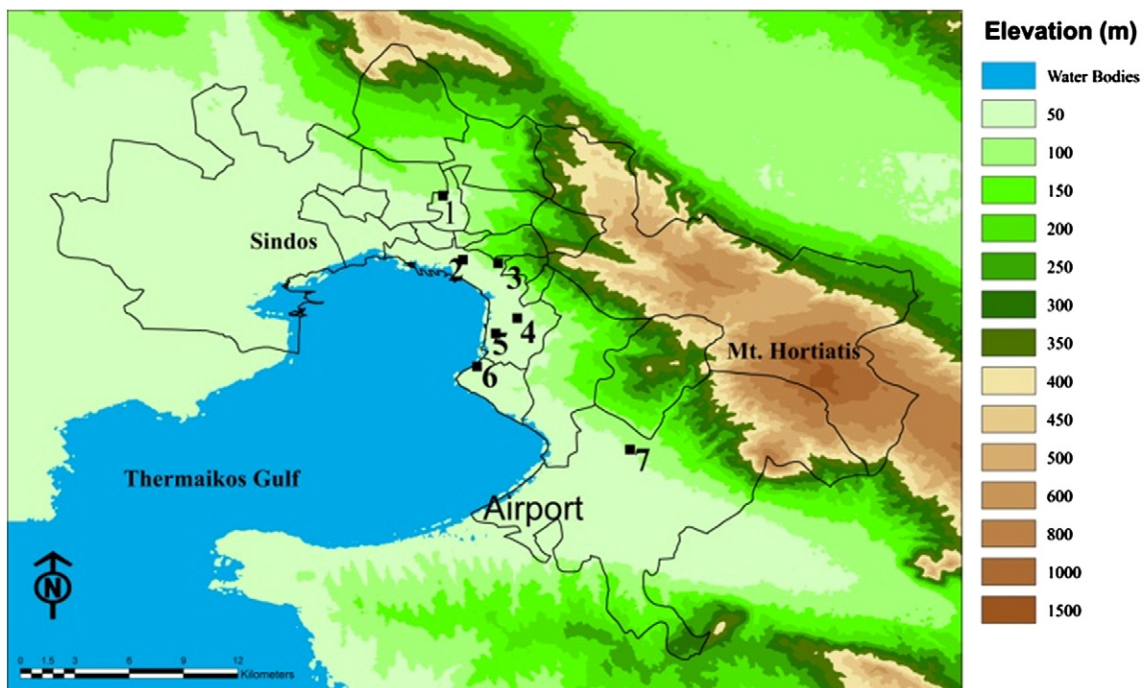


Fig. 1. The map of the study area. Squares indicate the locations of the meteorological shelters. Thessaloniki is divided in 19 sub-regions, which are demarcated by solid lines. Topography is shaded with linear altitude (above sea level) scales. The locations of Mount Hortiatis, industrial zone of Sindos, Thermaikos Gulf, and "Macedonia" International Airport are also shown.

**Table 1**
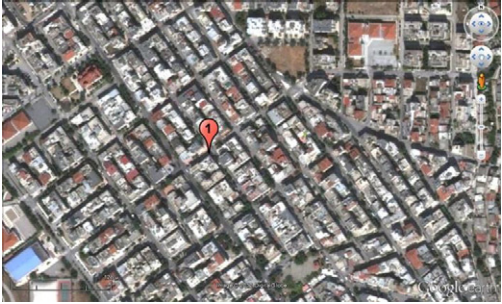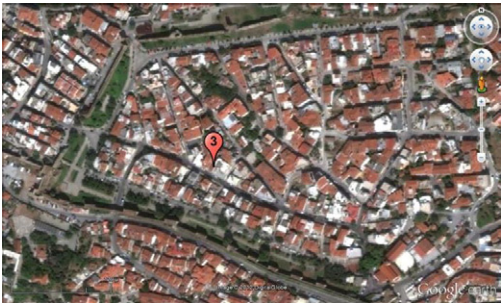Site characteristics for the seven measurement stations.

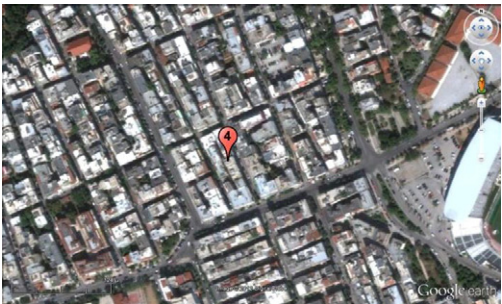| Station number | Abbreviation | Longitude (degrees east) | Latitude (degrees north) | Elevation[a] (m) | Description[b] | Green cover (%)[c] | Local Climate Zone[d] |
|---|---|---|---|---|---|---|---|
| 1 | SVP | 22° 55′ 40″ | 40° 40′ 30″ | 56 | | 1.3 | Compact midrise |
| 2 | AGD | 22° 56′ 22″ | 40° 38′ 34″ | 35 | | 1.2 | Compact midrise |
| 3 | ANP | 22° 57′ 25″ | 40° 38′ 34″ | 137 | | 3.1 | Compact lowrise |
| 4 | IPK | 22° 57′ 58″ | 40° 36′ 49″ | 32 | | 1.5 | Compact midrise |
| 5 | ANL | 22° 57′ 19″ | 40° 36′ 20″ | 14 | | 1.9 | Compact midrise |

**Table 1** (*continued*)

| Station number | Abbreviation | Longitude (degrees east) | Latitude (degrees north) | Elevation[a] (m) | Description[b] | Green cover (%)[c] | Local Climate Zone[d] |
|---|---|---|---|---|---|---|---|
| 6 | KLM | 22° 56′ 48″ | 40° 35′ 23″ | 27 |  | 2.1 | Open midrise |
| 7 | THR | 23° 01′ 23″ | 40° 32′ 54″ | 40 |  | 4.9 | Open lowrise |

[a]Elevation is provided relative to the mean sea level. [b]Image source: Google Earth. [c]Estimated according to Steeneveld et al. (2011) for a $300 \times 300$ m$^2$ area (representative of the neighbor scale in Thessaloniki). [d]Definition available in Stewart and Oke (2009a,b).

year (Melas et al., 1994). According to the early study of Sahsamanoglou (1976) the average frequency of sea breeze occurrence during the warm half of the year is 17 days per month.

## 2. Data sources and methodology

The data used in the present study are near-surface air temperatures measured at seven sites in the Thessaloniki metropolitan area during a 1-year period, spanning from March 2008 through February 2009. The selection of a full year of regular and repeated measurements ensures control over random variations and contributes towards the direction of obtaining representative results. At each measurement site, miniature data logging devices were used for recording air temperature and relative humidity. The technical specifications of the sensors and the loggers used are the following:

a) Manufacturer: Onset Computer Corporation.
b) Model name: HOBO U23-001.
c) Operation range: $-40\ °C$ to $70\ °C$ for the temperature sensor and 0 to 100% for the relative humidity sensor.
d) Accuracy: $\pm 0.2\ °C$ for the temperature sensor and $\pm 2.5\%$ for the relative humidity sensor.
e) Logger resolution: $0.02\ °C$ for the temperature sensor and 0.03% for the relative humidity sensor.
f) Data storage capacity: Over 42,000 of 12-bit measurements.

The accuracy of the experimental instrumentation is considered to be good and quite similar to measurement accuracies reported in previous studies (e.g. Livada et al., 2002; Steeneveld et al., 2011).

White shields, made of plastic, with lateral slots were used in order to protect the instruments from solar radiation and rain, and to allow for the natural ventilation of the instrumentation. To ensure consistency between the observations, the temperature and relative humidity sensors were calibrated by the Hellenic Institute of Metrology. The calibration procedure was conducted in laboratory conditions and revealed a negligible variability (~0.15 °C for air temperature and ~4% for relative humidity) between the HOBO sensors. The meteorological shelters were mounted on wooden brackets, 1.5 m long, and placed 3–5 m above the surface, and 4 m away from the nearest building wall, in suitably selected measurement sites. The data logging devices were configured to save air temperature and relative humidity data at 1-h intervals. It should be noted that since air temperature was measured at 3uses and land covers across the study area. Station 1 is located at the northwest boundary of Thessaloniki, close to the city's ring road, while station 2 is sited very near to the city center, on the major road of Agiou Dimitriou. Station 3 is located at the elevated old town of the city. Stations 4 and 5 can be found eastern of Thessaloniki's center, in areas that are not that highly influenced by traffic but are densely built-up. Station 6 was operated in the less densely built-up and populated area of Kalamaria, close to the eastern boundary of the city and very near to the coast of the Thermaikos gulf. Last, station 7 is located at the very east outskirts of the city, representing an area with low building density and abundant vegetation cover. Table 1 summarizes the characteristics of each measurement site. In overall, 6 stations could be characterized as urban (stations numbered 1–6), while 1 station could be considered to be representative of semi-rural conditions (station7).

All stations present a complete dataset of measurements for the period from March 2008 through February 2009. The selected year is considered to be a normal one, close to the previously reported climatology, since the mean annual temperature and relative humidity, averaged over all measurement sites, were found to be 17.4 °C and 63.6% respectively.

At this point, it is worth noticing that much effort has been put for the previously presented station setup and the analysis that follows, to comply with the standards recently set by Stewart (2011), concerning the representativity of UHI estimates. It is believed that the current study meets successfully 8 out of the 9 criteria defined in Stewart (2011) (i.e. conceptual model, operational definitions, instrument specifications, site metadata and representativeness, number of replicates, surface control, synchronicity), while it fails to comply with 1 criterion (i.e. weather control).

## 3. Results

### 3.1. Average air temperatures

The mean monthly air temperature values at each station are presented in Fig. 2. Results show that the maximum and minimum mean monthly temperatures are observed in August and in February, respectively. The higher monthly averaged values, ranging from 8.6 °C (February) to 29.5 °C (August), were recorded at station 2 that lies in the center of the city. The rest of the urban stations (stations 1, 3, 4, 5 and 6) were found to exhibit slightly lower temperatures (0.2 °C–0.5 °C) than

station 2. Not surprisingly, station 3 proved to be the coldest among the urban stations since it is located at the elevated area of the city that is characterized as a "compact lowrise" district with significantly higher amounts of vegetation than the rest of the stations found in the metropolitan area of Thessaloniki (Table 1). The lower mean monthly air temperatures, ranging from 7.1 °C (February) to 28.2 °C (August), were observed at semi-rural station 7 that is found at an "open lowrise" area in the distant east outskirts of the city (Table 1).

On the average monthly course, the urban/semi-rural temperature differences show very little seasonal variation, with slightly higher values during the colder months of the year. As it would be expected, the larger differences occur between stations 2 and 7 and range from 1.1 °C (June, September, and December) to 1.6 °C (October). The respective differences for the other urban stations are smaller and vary between 0.2 °C (station 3, September) to 1.4 °C (station 4, January). Station 3 in particular, shows the lowest temperature contrast to station 7 throughout the entire year. This could be attributed to the station's significantly higher elevation (Table 1). In addition, although station 3 is located within the larger urban zone of Thessaloniki, it shares common features with station 7. Both stations lie at areas characterized as "lowrise" with comparable vegetation cover fractions (Table 1).

The mean hourly air temperature values of each of the 7 examined stations are shown in Fig. 3a. Clearly, the maximum and minimum values are observed at noon hours, around 14–16 LT (LT = UTC + 2), and at early morning hours, around 06 LT, respectively. Station 2, located at the center of the city, exhibits the greatest maximum values, followed closely by surrounding urban station 1. Both stations are also characterized by the lowest percentages of green cover (Table 1) and can be thus considered to be the most built-up among all stations. Not surprisingly, the lowest maximum values are recorded in station 3 and are mainly due to the effect of elevation (Table 1). The lowest minimum values are detected in semi-rural station 7, while the greatest are observed in urban stations 2, 4 and 5.

Inspection of Fig. 3a reveals the distinct differences in the heating/cooling rates between the examined stations. Excluding station 3 that is situated at a significantly higher elevation than other stations, these differences can be in turn attributed to differences in the various fluxes of the urban/rural energy budget (e.g. heat storage) as discussed in Section 1. The release of heat storage is considered to be the most significant modification in the nocturnal urban energy balance, often exceeding in magnitude the radiative loss of a city (Christen and Vogt, 2004). In addition, the radiative cooling of urban areas is inhibited due to the surface enlargement that adds more surface for the re-absorption of the longwave radiation. Apparently, the results of the present study confirm this theory, as urban air temperatures remain higher than the concurrent values of semi-rural station 7 throughout the night.

Following sunrise (06 LT), the entire area of study begins to warm. The average urban and semi-rural heating rates during early morning hours (07–09 LT) were found equal to 0.4 °C/h and 0.7 °C/h (station averaged values), respectively. These values indicate that the semi-rural area represented by station 7 warms quicker than the city at the beginning of the day. This finding is consistent with the theory of UHI as stated

in Oke (1988; 1995) and has been also reported in previous heat island studies (e.g. Bassara et al., 2008; Lee and Baik, 2010). The slight lag between the urban and semi-rural data could be attributed to the complex urban geometry that now allows for a shading effect, inhibiting solar radiation from reaching the ground. Indeed, apart from station 3, all urban stations are found in areas characterized as either "compact midrise" or "open midrise". Christen and Vogt (2004) reported that the shading and exposure of the buildings significantly influences the penetration of solar radiation and, in turn, the availability of energy for heating.

As the day proceeds, heating continues and the recorded temperatures reach their maxima just after the time of solar peak, between 14 and 16 LT. The greatest maximum values are observed at stations 1 and 2, also occurring 1–2 earlier than the other stations. This could be attributed to the impact of anthropogenic heat that may form an important component of the local energy balance (Oke, 1982). It has also been reported that a major part of anthropogenic heat would originate from vehicles, in particular at areas crossed by major roads (Pigeon et al., 2007). Stations 1 and 2 lie at areas very near to major roads of the city and thus, it could be likely that heat released by vehicular traffic causes the increased maximum air temperatures. Unfortunately, since there were no measurements of energy fluxes available, the actual causes behind the different behavior of stations 1 and 2 cannot be speculated.

Following sunset (19 LT), the semi-rural surroundings of the city (station 7) begin to cool quickly. Conversely, the urban zone maintains higher air temperatures. According to Oke (1982), this thermal contrast results from the diverging urban/rural cooling rates. Despite the fact that most urban surfaces have higher emissivities than rural surfaces, the efficiency of radiative cooling is reduced due to the decreased sky view factor. Thermal properties (e.g. heat capacity, thermal conductivity) of urban materials are significantly different from soils and vegetated areas, also decreasing the cooling rate of urban areas. The slower urban cooling is further enhanced by the early evening release of stored heat (Christen and Vogt, 2004) and anthropogenic heat (Memon et al., 2009).

The greatest temperature differences are observed in nighttime hours, between 01 and 04 LT, approaching 2 °C and occurring between stations 5 and 7. On the other hand, the lowest differences are observed in early afternoon hours, between 15 and 17 LT, approaching 0.5 °C.
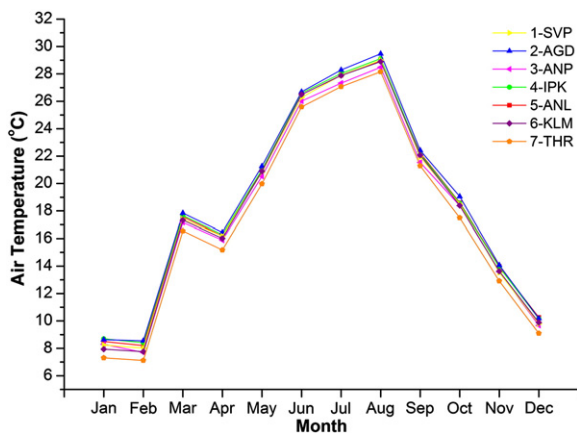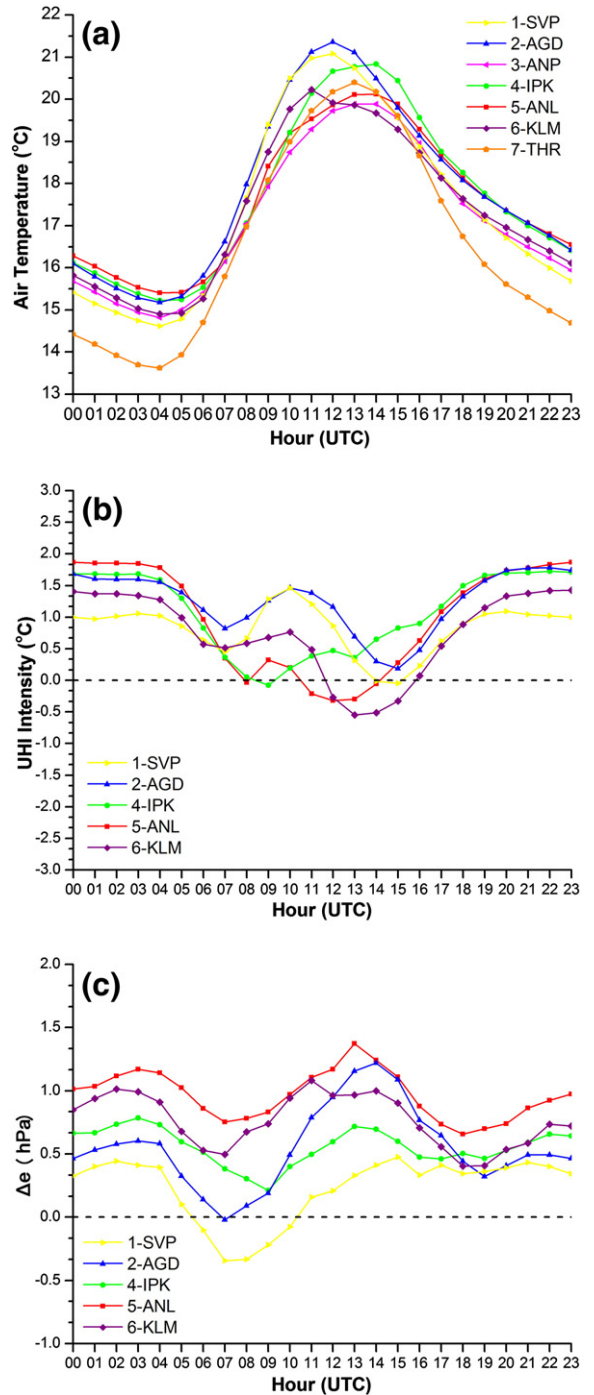


Fig. 3. Diurnal variation of mean hourly (a) air temperature, (b) urban heat island intensity, and (c) urban/rural water vapor pressure differences in the examined stations.



Fig. 2. Mean monthly air temperature in the examined stations.

*3.2. Urban heat island intensity*

The modification of air temperature in a city compared to the surrounding non-urbanized areas can be studied by comparing urban and suburban/rural stations that share similar topographic features. If the stations are near each other, then it can be assumed that their air temperatures would be the same as if there were no anthropogenic influence (Montavez et al., 2000). The examined urban and semi-rural stations appear to be suitable for carrying out such a comparison, excluding station 3 which is located at an elevated area.

According to Kim and Baik (2005), the intensity of an UHI (UHII) can be defined as the difference in air temperature between an urban and the surrounding suburban/rural area(s). In our study, the UHII can be defined as:

$$UHII = T_u(i) - T_r(i) \qquad (1)$$

where $T_u(i)$ is the temperature of the i-th urban station ($i = 1,2,4,5,6$) and $T_r$ is the temperature of the semi-rural station 7. As such, the temperature data of station 7 were subtracted from the respective temperature data of each urban station, in order to derive the intensity of the heat island in Thessaloniki. It is important to mention that there is in principle the possibility that the estimated UHII values be misinterpreted due to elevation differences between the reference station and the urban sites. However, the maximum elevation difference between station 7 and the urban sites approximates 25 m (Table 1). According to Stewart and Oke (2010), elevation changes of less than 30 m can be neglected as not influencing the local variations of air temperature. Indeed, assuming a moist adiabatic lapse rate of 6.5 °C/km, the resulting temperature correction for the above mentioned elevation difference approximates 0.17 °C; that is a rather small contribution to the intensity of the UHI.

At this point it is also worth clarifying the reasons behind the selection of station 7 as the reference one for computing the UHII, instead of the "Macedonia" International Airport whose data have been also used in the present study (Section 4.2). More importantly, the employment of temperature data from the "Macedonia" International Airport has been rejected due to them not being consistent with the temperature data collected by the measurement devices installed and operated in the metropolitan area of the city. As it has been already mentioned in Section 2, the temperature and relative humidity sensors that were installed in the greater Thessaloniki area have been calibrated to ensure consistency between the observations. Hence, it would not be proper to compare observations from different data logging devices (i.e. the HOBO sensors and the temperature sensor of the "Macedonia" International Airport) that have not been inter-calibrated. Furthermore, both station 7 and the "Macedonia" International airport lie near each other, at a distance of 15 km from the city center. As such, it can be considered that they actually represent the same geographical area.

To examine the characteristics of Thessaloniki's heat island, the estimated hourly UHII values were separated into four subsets, one for each season of the year. The first subset contains the hourly data for the summer months, June, July and August (JJA). The second one consists of the observations made during the autumn months, September, October and November (SON). The third contains the data collected during the winter months, December, January and February (DJF). The last subset consists of the hourly data recorded during the spring months, March, April and May (MAM).

Using the hourly heat island intensity values, the average values of the daily mean ($UHII_{mean}$), maximum ($UHII_{max}$) and minimum UHII ($UHII_{min}$) were calculated for every seasonal period (Table 2). In addition, a statistical analysis was conducted to examine the presence of statistically significant temporal trends between the considered seasonal periods, using the Mann-Kendall tau-statistic (Table 3). The null hypothesis ($H_o$) of the statistical analysis was set to that there is no variation and the calculated tau scores were tested at the significance level of 0.05 ($\alpha = 0.05$).

The data presented in Tables 2 and 3 suggest that a clear seasonal variation cannot be drawn on the basis of the season-averaged UHII values. However, there are indications that the UHI in Thessaloniki is more pronounced during the warm half of the year, as also noted in previous heat island studies (e.g. Klyzik and Fortuniak, 1999; Philandras et al., 1999; Morris et al., 2001). The largest $UHII_{max}$ values in 3 of the 5 urban sites occurred in JJA, while all stations showed the largest $UHII_{min}$ (in absolute values) during the same period. On average, the warmer MAM and JJA periods were characterized by higher $UHII_{max}$ and $UHII_{min}$ values at all stations. The decrease of the $UHII_{max}$ and $UHII_{min}$ values during the transition from summer to autumn is also confirmed by the larger, statistically significant, tau scores (Table 3).

The computed $UHII_{max}$ values are always greater than ~2 °C, approaching 3 °C in MAM and JJA periods (Table 2). The greatest $UHII_{max}$ values are observed at stations 2 and 4 that lie nearest to the city center (1 km and 2 km, respectively). The concentration of anthropogenic heat sources in the center of the city, especially central heating, could also be an explanation for the higher values recorded at both stations during the DJF period. Anthropogenic activity has also been used to explain UHII maxima in earlier studies (e.g. Giannaros et al., 2010; Jauregui, 1997; Papanastasiou and Kittas, 2011). On the other hand, the lowest values are found at station 6 that is located farther from the city center (6 km) in an area with lower building density ("open midrise") than other urban stations (Table 1).

The $UHII_{min}$ values are always negative, indicating that the examined urban sites are cooler than the semi-rural area represented by station 7 (Table 2). This implies that the city of Thessaloniki exhibits also the opposite to UHI phenomenon, the urban cool island (UCI). The $UHII_{min}$ values are larger (in absolute terms) during the MAM and JJA periods, suggesting an enhanced thermal contrast between the city and its surroundings. This enhanced thermal contrast must be driven by the availability of larger amounts of incoming solar radiation during the MAM and JJA periods than during the colder part of the year. This is supported by the fact that, as it will be later shown and discussed, $UHII_{min}$ values occur more frequently around the middle of the day when solar radiation dominates the surface energy budget.

It is worth noticing that the calculated differences agree rather well with previous heat island studies conducted in coastal cities. For instance, Papanastasiou and Kittas (2011)

**Table 2**
Season averaged values of daily mean, maximum and minimum UHII at each measurement station.

| Station | Daily mean (°C) | | | | Daily maximum (°C) | | | | Daily minimum (°C) | | | |
|---|---|---|---|---|---|---|---|---|---|---|---|---|
| | DJF | MAM | JJA | SON | DJF | MAM | JJA | SON | DJF | MAM | JJA | SON |
| 1 (SVP) | 0.8 | 0.8 | 0.8 | 0.8 | 2.4 | 2.5 | 2.5 | 2.2 | −0.4 | −0.8 | −1.2 | −0.7 |
| 2 (AGD) | 1.3 | 1.3 | 1.2 | 1.3 | 3.4 | 3.2 | 3.1 | 2.7 | −0.8 | −0.9 | −1.1 | −0.3 |
| 4 (IPK) | 1.2 | 1.1 | 1.0 | 1.0 | 3.3 | 2.9 | 2.7 | 2.3 | −0.8 | −1.0 | −1.1 | −0.6 |
| 5 (ANL) | 1.2 | 1.0 | 0.8 | 1.0 | 2.5 | 2.7 | 2.9 | 2.4 | −0.4 | −1.0 | −1.4 | −0.7 |
| 6 (KLM) | 0.7 | 0.7 | 0.8 | 0.8 | 1.9 | 2.3 | 2.5 | 2.1 | −0.7 | −1.1 | −1.3 | −0.8 |

reported that the average maximum UHII in Volos, Greece, is 2 °C.

The frequency distribution of the estimated average values for the daily maximum UHII and for the specified seasonal periods is shown in Fig. 4. The calculated daily maximum UHII values appear to follow a skewed distribution as proposed in earlier studies (e.g. Lee and Baik, 2010; Steeneveld et al., 2011). During the hot period of the year (March to August), the maximum intensity of the UHI is more probable to be greater than 2 °C and lower than 4 °C. Conversely, during the colder part of the year (September to February), daily maximum UHII values are more likely to be greater than 1 °C and lower than 3 °C. Looking at Fig. 4, one can also notice that UHII values greater than 4 °C can be also observed during the coldest DJF period with decreasing frequencies. In other words, the UHI in Thessaloniki can be more clearly observed during the warm part of the year (MAM, JJA), but extreme UHII values are more likely to be detected during the colder months (DJF).

An important factor that should be also included at this juncture of discussion is the impact of synoptic scale weather conditions on UHI magnitude. For instance, the UHII has been proven to be greatest during anticyclonic conditions (e.g. Morris and Simmonds, 2000; Kassomenos and Katsoulis, 2006). Seemingly, this is generally confirmed by the results from Thessaloniki. Higher UHII values were observed during the warmer months when the synoptic scale weather is dominated by stable circulation types (Maheras et al., 2000).

Fig. 5a depicts the frequency distribution of the time of occurrence of the daily maximum UHII. More than half of the estimated maximum temperature differences are detected during night hours (from 20 to 06 LT), irrespective of the examined seasonal period. In particular, maximum UHII values are usually observed following sunset, when the greater heat storage in the urban zone results to maintaining elevated temperatures in the center of the city.

On the other hand, the number of recorded maxima of UHII during solar peak hours (from 12 to 16 LT) is significantly low (<17%), especially during the JJA and SON periods. This becomes more evident looking at Fig. 5b which depicts the frequency distribution of the time of occurrence of the daily minimum UHII. Irrespective of the seasonal period, more than 40% of the daily minimum UHII values are observed between 12 and 16 LT. During these hours the energy budget of the measurement sites is dominated by the presence of a huge source of heating, the sun, resulting to a sharp reduction in the respective temperature differences.

On the average diurnal course, the UHI impact is found to be more pronounced during the night than during the day

(Fig. 3b), as noted in previous heat island studies (e.g. Bassara et al., 2008; Memon et al., 2009). Clearly, the heat island starts developing in the late afternoon hours (17–18 LT) as a result of the increasing and significantly greater release of heat storage in the urban areas (Christen and Vogt, 2004). Its intensity reaches a maximum plateau during the night (00–05 LT), before decreasing abruptly following sunrise.

The emergence of sun must be the cause behind the abrupt decrease in the UHII that is observed in early morning hours. At the beginning of the day the urban and rural energy budget is dominated by the absorption of the incoming solar radiation. Since the source of heat is the same for both areas, it is expected that the urban/rural thermal contrast be diminished. Seemingly, the results for Thessaloniki confirm this, as a rapid decrease in the UHII can be observed following sunrise. As the day proceeds, the release of heat by anthropogenic sources (e.g. traffic) becomes important. As a result, an increase in the UHII during morning hours, when traffic load is higher, can be seen in Fig. 3b. According to Pigeon et al. (2007), a major part of anthropogenic heat would originate from road traffic, especially in areas crossed by major roads. Since stations 1 and 2 are both located at areas very near to major roads of the city, it is possible that the greater UHII increase is due to the heat released by vehicular traffic. According to Memon et al. (2009) heat released by vehicles would have a considerable and direct impact on air temperature.

During the solar peak time (11–14 LT) the entire study area stores heat to its full capacity by absorbing the incoming solar radiation, while the resulting heat surplus is partitioned to the latent and sensible heat fluxes. However, urban surfaces are

**Table 3**
Mann–Kendall tau statistic of the season averaged daily mean, maximum and minimum UHII at each measurement station. Values typeset in bold indicate statistically significant trends (α = 0.05).

| Daily mean (°C) | 1(SVP) | 2(AGD) | 4(IPK) | 5(ANL) | 6(KLM) |
|---|---|---|---|---|---|
| DJF to MAM | −0.02 | 0.05 | −0.04 | −0.07 | **0.10** |
| MAM to JJA | **−0.10** | 0.02 | −0.10 | −0.11 | 0.02 |
| JJA to SON | −0.04 | 0.05 | −0.01 | **0.15** | −0.09 |
| SON to DJF | 0.08 | −0.02 | **0.17** | **0.12** | −0.11 |
| Daily maximum (°C) | | | | | |
| DJF to MAM | −0.05 | 0.09 | −0.02 | **0.24** | **0.29** |
| MAM to JJA | **−0.11** | 0.01 | −0.06 | −0.01 | −0.02 |
| JJA to SON | **−0.11** | **−0.22** | **−0.21** | **−0.28** | **−0.26** |
| SON to DJF | 0.08 | **0.17** | **0.31** | 0.03 | −0.08 |
| Daily minimum (°C) | | | | | |
| DJF to MAM | −0.08 | −0.09 | **−0.16** | **−0.26** | **−0.18** |
| MAM to JJA | **−0.12** | −0.07 | −0.03 | −0.05 | −0.03 |
| JJA to SON | **0.20** | **0.26** | **0.24** | **0.24** | **0.19** |
| SON to DJF | **0.20** | −0.02 | 0.08 | **0.18** | 0.09 |

able to store more heat, resulting to a significantly greater storage heat flux as compared to rural areas, especially during the midday hours (Christen and Vogt, 2004; Oke, 1988). As more heat is removed from the urban atmosphere through the storage heat flux, it would be expected that the intensity of the heat island decrease. This is true for Thessaloniki, where a drop in the UHII can be seen during the afternoon hours.

More interestingly, the results indicate that in the late afternoon the metropolitan area of the city behaves like an urban cool island (UCI). This has been also observed in the recent study of Kantzioura et al. (2012), while the development of a reversed UHI during the midday and late afternoon hours has been also recorded in other parts of the world (e.g. Alonso et al., 2003; Bassara et al., 2008; Memon et al., 2009; Shigeta et al., 2009; ). Memon et al. (2009) suggest that the causes behind the negative UHII values include the attenuation of the incoming solar radiation due to the polluted urban atmosphere, the shading effect of buildings, and the significantly greater urban storage heat flux.

Looking at Fig. 3b, one can finally notice that the lower mean hourly UHII values are observed in stations 1 and 6. Both stations lie at the boundaries of the urban zone of the city, in less densely built-up areas. Station 6 in particular, is located at an "open midrise" area with higher vegetation cover than other urban stations considered in this analysis (Table 1) and is also expected to be influenced by the development of the sea breeze. As such, the advection of cooler marine air, especially in afternoon and evening hours when the sea breeze is generally stronger, would result to lowering air temperature.

The frequency distribution of the hourly UHII values, considering all stations, is presented in Table 4. In the annual course, the more frequent class of UHII values is (0,1] (31.7%), while the total percentage of negative UHII values is found to be equal to 18.5%.

During the warm period of the year (JJA and MAM), nearly 22% of the UHII observations yield a value greater than 2 °C, with approximately 3% greater than 3 °C. For the same seasonal periods, approximately 20% of the observations are found to be associated with UHII values lower than 0 °C. During the transitional SON period the percentage of UHII observations with a value greater than 2 °C is reduced to about 14%. On
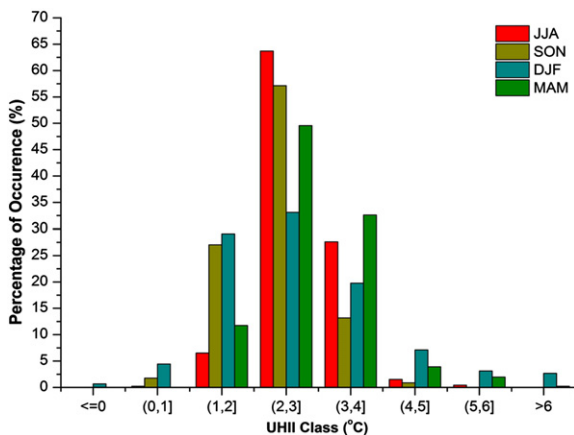
the other hand, winter presents the most UHII values greater than 3 °C (~8%). The above results are in good agreement with the recent study of Poupkou et al. (2011), reporting higher frequencies for UHII values greater than 0 °C and lower than 3 °C.

## 4. Discussion

### 4.1. Impact of moisture availability

It is well known that air humidity plays an important role in the urban energy balance (e.g. Oke, 1982; Weber and Kuttler, 2005). Furthermore, several previous studies have shown that humidity differences between urban and rural areas exist (e.g. Ackerman, 1971; Chandler, 1967; Hage, 1975; Jauregui and Tejeda, 1997; Lee, 1991). Although cities are generally considered to be drier than their surrounding non-urbanized areas, higher urban humidity levels have been reported in several previous studies (e.g. Fortuniak et al., 2006; Hage, 1975; Kuttler et al., 2007). These positive urban/rural vapor pressure differences indicate that an urban area is moister than its rural surroundings, an effect that is known as the urban moisture excess (UME) (e.g. Kuttler et al., 2007).

Different causes for the development of the UME are discussed in literature, but there are only a few studies quantifying the processes they identified for UME development. However, there is consensus that evaporation, condensation, advection and anthropogenic emissions of water vapor contribute to the formation of urban/rural humidity differences (Holmer and Eliasson, 1999). For instance, Chandler (1967) and Hage (1975) reported that continued evaporation in the city during the night is responsible for the nocturnal UME, whereas early morning dewfall removes vapor from the atmosphere to the surface in rural areas.

One interesting question is how the UME interacts with the development of the UHI. As early as in 1991, Lee (1991) reported a good positive correlation between the mean monthly vapor pressure difference and the mean monthly UHII for London, but he considered the higher urban humidity levels to be only an effect of the UHI. However, Holmer and Eliasson (1999) demonstrated that the UME could also induce a significant impact on UHI development.

In the present study, water vapor pressure differences (Δe) between the urban sites and the reference site were used to investigate the connection between the UHI formation and moisture availability. Hourly water vapor pressure data were derived from the air temperature and relative humidity measurements. First, the saturation vapor pressure was computed using the Goff–Gratch equation (WMO, 2000); the vapor pressure was subsequently calculated using the measured relative humidity.

On the average daily course the urban area of Thessaloniki is found to be moister than its semi-rural surroundings (station 7) (Fig. 3c), in particular during the night. The observed diurnal variation with the generally larger urban excess during the night, the rapid decrease in Δe following sunrise, and the afternoon maxima agrees well with results presented by Hage (1975), Ackerman (1987), and Holmer and Eliasson (1999). The computed maximum mean vapor pressure differences (>0.5 hPa on average) correspond to an intense UME (Kuttler et al., 2007).
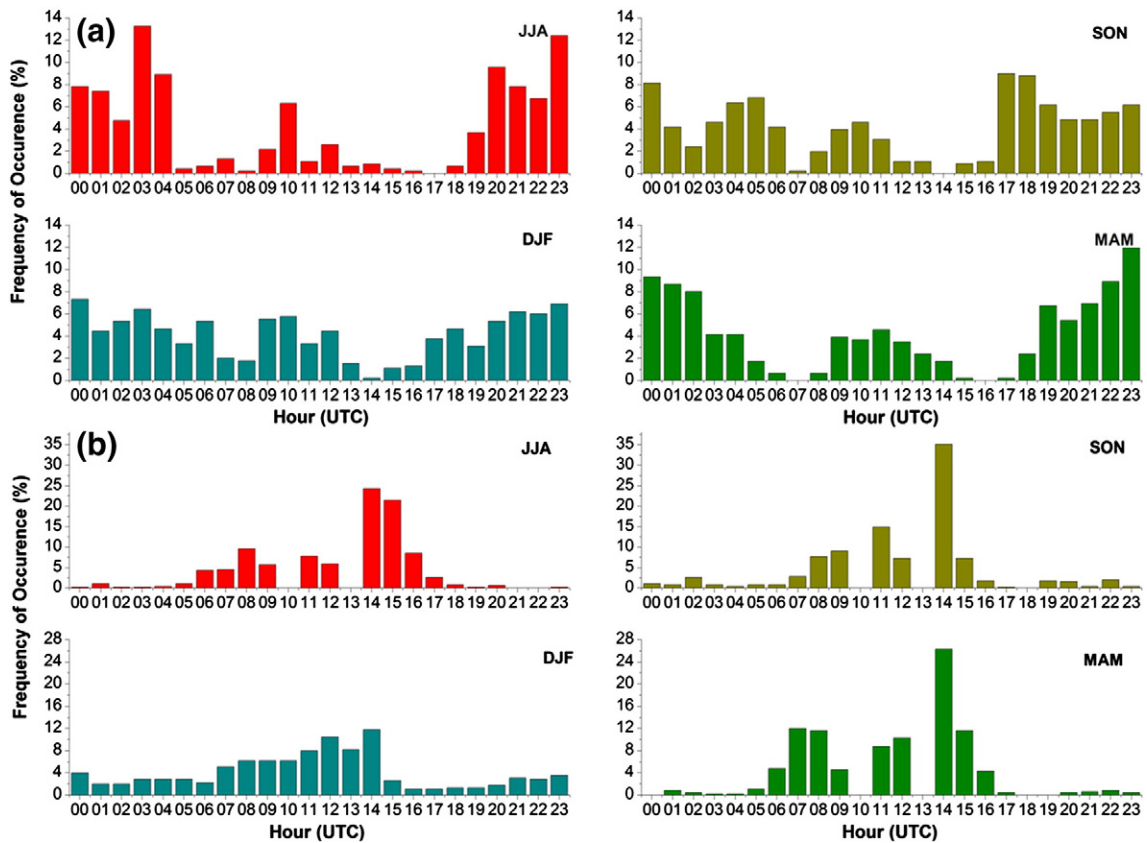


**Fig. 4.** Frequency distribution of the daily maximum UHII values for the different seasonal periods in all examined stations.

**Fig. 5.** Frequency distribution of the time of occurrence of (a) the daily maximum UHII (top panel) and (b) the daily minimum UHII (bottom panel) for the different seasonal periods in all examined stations.

The analysis of the mean diurnal patterns of Δe and UHII reveals that the UHI precedes the UME during the night. The maximum intensity of the UHI occurs around midnight, which is 4–6 h before the maximum nighttime vapor pressure difference is observed. This indicates that the elevated temperatures due to the nocturnal UHI cause continued evaporation and reduced condensation in the urban areas, as earlier studies assumed (e.g. Chandler, 1967; Hage, 1975; Lee, 1991; Holmer and Eliasson, 1999). At the same time evaporation in the semi-rural site is expected to be considerably hindered by the decrease of air temperature due to the greater radiative loss. As a result, vapor often condensates on the

surface in the form of dew that evaporates quickly after sunrise, causing the sudden morning decrease in Δe (Fig. 3c).

The above findings are further supported by the linear regression between the nocturnal mean hourly UHII and Δe values (Fig. 6a). Although the computed correlation coefficient (r = 0.5) could be considered to be low, it becomes significant taking into account the previously discussed phase shift. It indicates that the nocturnal heat island plays an important role in shaping the vapor pressure differences, causing the moisture excess in the urban areas. The significance of this relation is further supported by the low p value (<0.001) that was computed using the two-tailed t-statistic.

Contradictory results are obtained when examining the mean daytime patterns of Δe and UHII. Closer examination of Fig. 3b and c reveals that daytime UHII and Δe values are rather anti-correlated, contrary to what was observed during the night. In particular, vapor pressure differences are found to increase in the afternoon, whereas the intensity of the heat island decreases. This could be attributed to the influence of the sea breeze that allows for the transport of humid maritime air over the urban areas of Thessaloniki. Due to the coastline orientation of the city it is expected that the urban areas be affected by the sea breeze circulation more directly and at a greater extent than the semi-rural area represented by station 7, as shown in previous studies (Melas et al., 1994; Moussiopoulos et al., 2006). However, it remains

**Table 4**
Frequency distribution of the hourly UHII observations within various ranges for the specified seasonal periods. Parentheses denote > and brackets denote ≤.

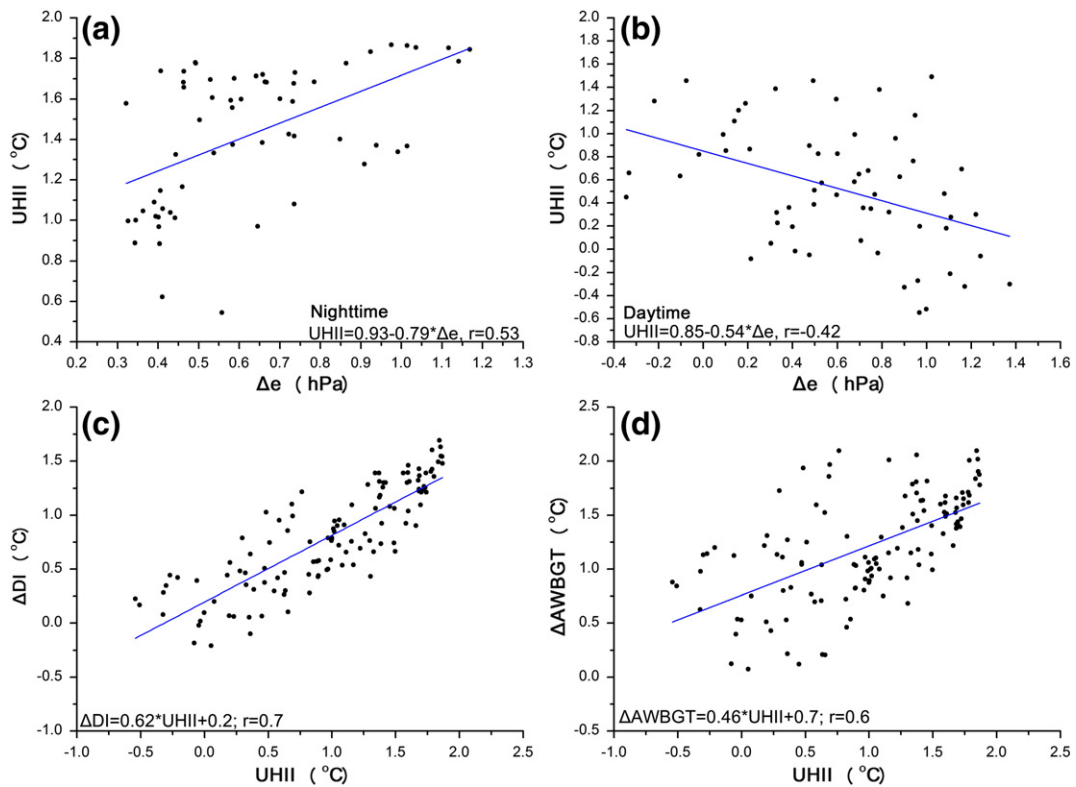| Period | UHII ranges (°C) | | | | | |
|---|---|---|---|---|---|---|
| | ≤−1 | (−1,0] | (0,1] | (1,2] | (2,3] | >3 |
| Annual | 6.2 | 12.3 | 31.7 | 30.2 | 15.3 | 4.4 |
| Summer (JJA) | 7.0 | 15.2 | 26.6 | 29.5 | 19.4 | 2.4 |
| Autumn (SON) | 2.9 | 12.0 | 35.8 | 35.0 | 13.2 | 1.2 |
| Winter (DJF) | 6.4 | 9.5 | 35.5 | 28.3 | 12.5 | 7.7 |
| Spring (MAM) | 6.3 | 12.6 | 29.1 | 30.7 | 17.4 | 3.9 |

**Fig. 6.** Linear regression analysis between (a) nighttime mean hourly UHII values and water vapor pressure differences (the typical uncertainty for the estimated UHII and Δe data is 0.34 °C and 0.23 hPa, respectively), (b) daytime mean hourly UHII values and water vapor pressure differences (the typical uncertainty for the estimated UHII and Δe data is 0.53 °C and 0.41 hPa, respectively), (c) mean hourly UHII values and discomfort index differences (the typical uncertainty for the estimated UHII and ΔDI data is 0.82 °C and 0.67 °C, respectively), and (d) mean hourly UHII values and approximated wet bulb globe temperature differences (the typical uncertainty for the estimated UHII and ΔAWBGT data is 0.82 °C and 1.04 °C, respectively).

for the future to quantify the impact of the sea breeze on the formation of the UME in Thessaloniki. Another contributing factor to the daytime UME could also be the diurnal pattern of rainfall. According to the early study of Giles and Flocas (1990), Thessaloniki has a marked maximum rainfall during the afternoon, on an annual basis.

The results of the regression analysis between the daytime mean hourly UHII and Δe values support the above likely explanation (Fig. 6b). Daytime temperature and vapor pressure differences are found to be negatively correlated ($r = -0.4$). The significance of this correlation is confirmed by the two-tailed $t$-test with $p < 0.001$. An important factor that should be taken into account at this point is the impact of the observed moisture excess on the intensity of the heat island. Holmer and Eliasson (1999) showed that the UME has a pronounced effect on the latent vapor fluxes, counteracting the development of the UHI. This appears to be confirmed in the case of Thessaloniki, where the increasing UME intensity results to decreasing UHII values.

### 4.2. Impact of wind conditions

According to Figuerola and Mazzeo (1999), and Kidder and Essenwanger (1995), wind speed is one of the most significant meteorological factors that influence the development and the intensity of the UHI effect. Therefore, a separate

analysis is carried out in order to examine the impact of the wind on the heat island of Thessaloniki. The analysis is carried out during the specified seasonal periods, using wind velocity data retrieved from the meteorological station of the "Macedonia" International Airport of Thessaloniki. The temporal resolution of the wind data is hourly, coinciding with the temporal resolution of the air temperature and relative humidity data.

Five meteorological wind speed ranges were defined, from below 2 m/s to above 8 m/s (interval set to 2 m/s). Since this study considers wind data from the meteorological station of the "Macedonia" airport, one could expect lower wind velocities in the urban zone of the city.

During the transitional MAM and SON periods around 70% of the observations showed a wind speed value lower than 4 m/s, while for the JJA and DJF periods the corresponding percentages were ~50% and ~60%, respectively. Higher wind velocities (greater than 6 m/s) are more probable to be observed during the summer and winter season, with winter presenting the largest percentage of wind speed values greater than 8 m/s (~11%).

The frequency distribution of the hourly UHII values within the specified wind speed ranges for all stations is presented in Table 5. Clearly, UHII values greater than 2 °C are more probable to be detected when wind speed is below 4 m/s. Considering the first two wind speed ranges (i.e. wind

speed values lower than 4 m/s), the percentage of UHII observations that yield a value greater than 2 °C is around 25%, with approximately 5% greater than 3 °C. Under the same wind conditions, 10–15% of the observations are found to be associated with negative UHII values. On the other hand, high wind velocities (above 6 m/s) appear to reduce significantly the intensity of the UHI. Considering the last two wind speed ranges (i.e. wind speed values greater than 6 m/s), the percentage of UHII values lower than 1 °C is found to be ~70%, with 20–30% yielding a UHII value lower than 0 °C. Similar results were also reported for Athens, Greece, in the study of Kassomenos and Katsoulis (2006).

Table 6 presents the average UHII values that were computed for every wind speed range and for the different seasonal periods. It is clear that there is a gradual decrease of UHII with increasing wind speed, irrespective of the examined seasonal period. It can be seen that the largest UHII values are observed when wind is weak (below 2 m/s), while the minimum values are found when wind velocities exceed 6 m/s. It is also worth noticing that the critical wind speed value, above which the intensity of the UHI is significantly reduced, equals 4 m/s.

### 4.3. Impact of the UHI on thermal comfort

The data analysis that was presented in the previous sections revealed that the heat island of Thessaloniki is more pronounced in summer months, and is strongest during nighttime hours. Furthermore, it was shown that the UHI correlates rather well with the UME. Therefore, it would be of interest to investigate the impact of the UHI on thermal comfort conditions. To this end, the hourly values of the discomfort index (DI) and the approximated wet bulb globe temperature (AWBGT) were calculated for the summer subset (JJA) of the entire dataset.

DI, which was originally proposed by Thom (1959), is a simple and well documented index of thermal comfort. It can be calculated using Eq. (2):

$$DI = T_a - 0.55 * (1 - 0.01 * RH) * (T_a - 14.5) \qquad (2)$$

where $T_a$ is the air temperature (°C) and RH is the relative humidity (%). When DI ≤ 21 °C no discomfort is expected. For 21 °C < DI ≤ 24 °C less than half of the population is expected to feel discomfort, while for 24 °C < DI ≤ 27 °C the anticipated percentage of the population feeling discomfort rises to above 50%. The majority of the population is expected to feel

**Table 5**
Frequency distribution of the hourly UHII observations within various temperature and wind speed ranges. Parentheses denote > and brackets denote ≤.

| Wind speed range (m/s) | UHII ranges (°C) | | | | | |
|---|---|---|---|---|---|---|
| | ≤ −1 | (−1,0] | (0,1] | (1,2] | (2,3] | > 3 |
| < 2 | 2.6 | 6.5 | 25.7 | 39.6 | 20.9 | 4.5 |
| [2,4) | 4.9 | 10.6 | 26.9 | 31.3 | 21.3 | 5.0 |
| [4,6) | 9.9 | 20.4 | 39.0 | 22.8 | 6.0 | 1.9 |
| [6,8) | 10.4 | 19.4 | 44.5 | 19.3 | 4.7 | 1.7 |
| ≥ 8 | 4.9 | 14.7 | 50.7 | 23.8 | 3.9 | 2.0 |

**Table 6**
Average UHII values under different wind speed ranges for the specified seasonal periods. Parentheses denote < and brackets denote ≥.

| Station | Wind speed range (m/s) | | | | |
|---|---|---|---|---|---|
| | < 2 | [2,4) | [4,6) | [6,8) | ≥ 8 |
| 1 (SVP) | 1.2[a] | 1.1 | 0.5 | 0.1 | 0.5 |
| | 0.9[b] | 0.9 | 0.4 | 0.2 | 0.5 |
| | 1.2[c] | 1.0 | 0.5 | 0.3 | 0.6 |
| | 1.1[d] | 1.1 | 0.7 | 0.4 | 0.6 |
| 2 (AGD) | 1.8 | 1.6 | 0.7 | 0.5 | 1.0 |
| | 1.5 | 1.4 | 0.8 | 0.7 | 1.1 |
| | 1.7 | 1.7 | 0.6 | 0.3 | 1.0 |
| | 1.6 | 1.4 | 0.8 | 0.7 | 0.9 |
| 4 (IPK) | 1.6 | 1.2 | 0.4 | 0.8 | 0.8 |
| | 1.3 | 1.0 | 0.4 | 0.6 | 0.7 |
| | 1.7 | 1.6 | 0.7 | 0.2 | 0.9 |
| | 1.3 | 1.1 | 0.6 | 0.8 | 0.9 |
| 5 (ANL) | 1.7 | 1.2 | 0.0 | 0.3 | 0.7 |
| | 1.4 | 1.1 | 0.4 | 0.6 | 0.9 |
| | 1.3 | 1.3 | 0.9 | 0.8 | 0.9 |
| | 1.4 | 1.0 | 0.3 | 0.5 | 0.8 |
| 6 (KLM) | 1.4 | 1.3 | 0.3 | − 0.1 | 0.2 |
| | 1.1 | 0.9 | 0.3 | 0.3 | 0.6 |
| | 0.8 | 0.9 | 0.5 | 0.3 | 0.6 |
| | 1.1 | 1.0 | 0.2 | 0.1 | 0.4 |

[a] JJA; [b] SON; [c] DJF; [d] MAM.

discomfort when 27 °C < DI ≤ 29 °C, and the entire population experiences heavy discomfort when 29 °C < DI ≤ 32 °C. A DI > 32 °C represents sanitary emergency conditions.

In addition to DI, the AWBGT was computed by applying Eq. (3) (Steeneveld et al., 2011):

$$AWBGT = 0.567 * T_a + 0.393 * e + 3.94 \qquad (3)$$

where $T_a$ is the air temperature (°C) and e the water vapor pressure (hPa). Contrary to DI, the threshold values of AWBGT depend largely on personal clothing and level of activity. In order to interpret the calculated AWBGT values for Thessaloniki, a general classification scheme is adopted as proposed in Steeneveld et al. (2011). A AWBGT < 27.7 °C represents absence of heat stress. For 27.7 °C < AWBGT < 32.2 °C heat stress increases, while for AWBGT > 32.2 °C great heat stress danger occurs.

At a first stage, the mean DI and AWBGT values were calculated for every month of the summer period and for each of the examined stations (except from station 3 which was also excluded from the UHII analysis). Results are presented in Table 7. Clearly, higher DI and AWBGT values are observed in August which was also proved to be the hottest month of the year (Fig. 2). As it would be expected, the station that lies at the heart of the city (station 2) exhibits the highest DI and AWBGT values. On the other hand, the lowest values are detected in surrounding urban station 1 and in semi-rural station 7. Apparently, throughout the entire JJA period both stations present DI values which indicate that less than half of the population is expected to feel discomfort, while heat stress danger is also found to be low (AWBGT < 27.7 °C). Conversely, the computed DI values for the rest of the stations exceed 24 °C (Jul and Aug), indicating that more than half of the population is expected to be feel discomfort.

Fig. 7 depicts the diurnal cycle of DI and AWBGT in the selected urban and semi-rural stations. The observed diurnal march of both indices appears to follow closely the one of air temperature (Fig. 2). The feeling of discomfort and heat stress risk appears to be minimum around the time of sunrise (06 LT), while higher values are observed at early afternoon hours (14–15 LT). This diurnal march agrees well with the one reported in the early study of Angouridakis and Makrogiannis (1982), presenting the climatology of DI in the center of Thessaloniki for the years 1950–1975. More recently, Papanastasiou et al. (2010) presented a similar daily variation for DI in the coastal city of Volos, Greece.

Closer examination of Fig. 7 reveals one interesting feature. All urban stations exhibit mean hourly DI values greater than 24 °C for a prolonged time period of 11–12 h (from ~09 to ~2 LT). Meanwhile, urban AWBGT values exceed 27.7 °C during 8–9 h. This indicates that a great part of the population living in the examined areas is expected to be subject to discomfort and heat stress conditions during most hours of the day. Moreover, it can be observed that the feeling of discomfort and heat stress is more pronounced in the area of station 2 during early afternoon hours (14–15 LT), when DI and AWBGT values approximate 27 °C and 30 °C, respectively.

On the other hand, the recorded DI and AWBGT values in semi-rural station 7 indicate that people living in this area are less affected by discomfort and heat stress conditions. More precisely, DI values appear to exceed 24 °C for a time period of no more than 9 h (from 11 to 19 LT), with peak values (still lower than 25.5 °C) being observed in early afternoon hours (i.e. from 14 to 17 LT). Heat stress conditions are found worse for a shorter period of 5 h in the afternoon (13 to 17 LT) when AWBGT values approximate 28 °C.

Table 8 presents the frequency distribution of the hourly DI and AWBGT values at all examined stations. It can be seen the percentages of the hourly DI values falling in class 2 (i.e. (24,27]) exceed 45% in the urban stations, whereas in the semi-rural station 7 the respective percentage drops to about 37%. AWBGT values are also more frequently higher than 27.7 °C in the urban sites (above 40% on average) than in the semi-rural area of station 7 (~30%). The densely built-up area that is represented by station 2 appears to be more prone to higher DI values. Nearly 60% of the DI observations in station 2 exceed 24 °C, with 11% being greater than 27 °C. With regards to heat stress conditions, station 2 also shows the greatest percentage of hourly AWBGT values greater than 32.2 °C (3.7%).
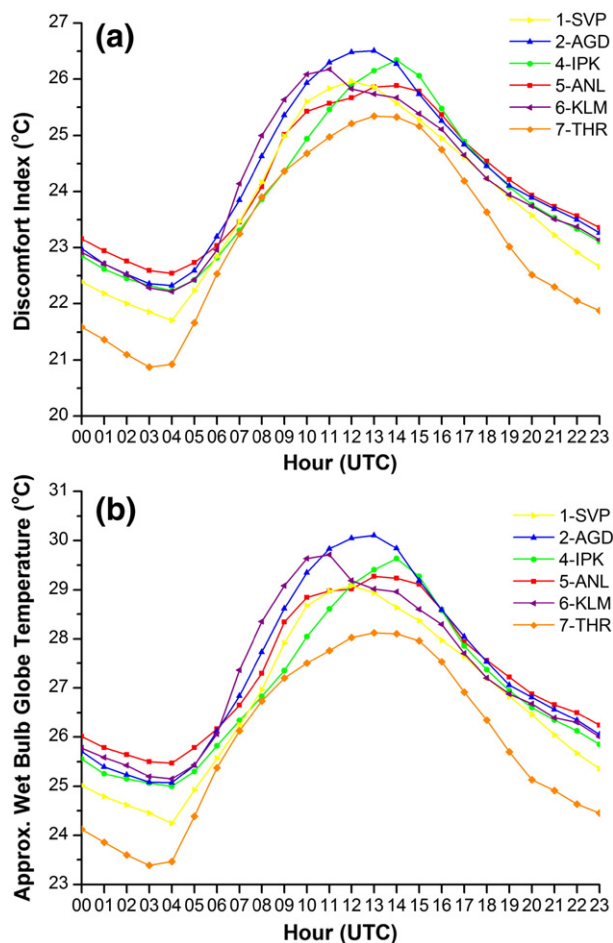


**Fig. 7.** Diurnal variation of mean hourly (a) discomfort index, and (b) approximated wet bulb globe temperature in the examined stations during the JJA period.

On the other hand, nearly 11% and 16% of DI observations are lower than 21 °C in stations 1 and 7, respectively. Both stations also exhibit the greatest percentages of occurrence for AWBGT ≤ 27.7 °C (62.8% and 70.5%, respectively). The corresponding percentages appear to decrease moving towards the city center (station 2). This indicates that people living closer to the center of Thessaloniki are less probable to obtain relief from heat stress and discomfort conditions.

It is worth noticing that the above findings concerning the distribution of DI values in the urban agglomeration of Thessaloniki are generally in good agreement with the previous study of Poupkou et al. (2011). However, in the present study it is most frequent that more than 50% of the urban population feels discomfort (third DI class), while according to Poupkou et al. (2011) this percentage is lower than 50% (second DI class).

To examine the influence the UHI may have on discomfort, a linear regression analysis between UHII and the DI and AWBGT differences was carried out, considering the entire summer dataset of observations. The hourly DI and AWBGT differences (ΔDI, ΔAWBGT), which were used for deriving the mean hourly values, were calculated by subtracting

**Table 7**
Mean monthly DI and AWBGT values at each measurement station for every month of the JJA period.

| Station | DI (°C) | | | AWBGT (°C) | | |
|---|---|---|---|---|---|---|
| | Jun | Jul | Aug | Jun | Jul | Aug |
| 1 (SVP) | 23.0 | 23.9 | 24.0 | 25.9 | 26.7 | 27.5 |
| 2 (AGD) | 23.4 | 24.3 | 25.1 | 26.4 | 27.3 | 28.3 |
| 4 (IPK) | 23.3 | 24.1 | 24.7 | 26.2 | 26.9 | 27.7 |
| 5 (ANL) | 23.4 | 24.2 | 24.9 | 26.5 | 27.2 | 28.1 |
| 6 (KLM) | 23.4 | 24.2 | 24.8 | 26.5 | 27.2 | 28.0 |
| 7 (THR) | 22.4 | 23.4 | 24.0 | 24.8 | 26.1 | 26.8 |

**Table 8**
Frequency distribution of the hourly DI and AWBGT observations at each measurement station within the specified DI and AWBGT ranges.

| Station | DI classes (°C) | | | | | | AWGBT classes (°C) | | |
|---|---|---|---|---|---|---|---|---|---|
| | ≤21 | (21,24] | (24,27] | (27,29] | (29,31] | >31 | ≤27.7 | (27.7,32.2] | >32.2 |
| 1 (SVP) | 10.9 | 39.9 | 43.9 | 5.3 | 0.0 | 0.0 | 62.8 | 36.8 | 0.4 |
| 2 (AGD) | 9.0 | 33.1 | 46.6 | 10.9 | 0.4 | 0.0 | 53.8 | 42.6 | 3.7 |
| 4 (IPK) | 9.3 | 37.1 | 46.4 | 7.1 | 0.1 | 0.0 | 58.9 | 39.9 | 1.2 |
| 5 (ANL) | 8.0 | 34.7 | 51.0 | 6.3 | 0.0 | 0.0 | 53.9 | 44.5 | 1.6 |
| 6 (KLM) | 9.2 | 34.9 | 47.4 | 8.5 | 0.1 | 0.0 | 54.8 | 43.6 | 1.6 |
| 7 (THR) | 16.1 | 43.3 | 37.2 | 3.4 | 0.0 | 0.0 | 70.5 | 29.5 | 0.0 |

the hourly DI and AWBGT value of semi-rural station 7 from that of the urban stations. A positive ΔDI or ΔAWBGT value indicates that the feeling of discomfort or heat stress, respectively, is stronger in the urban areas of the city.

The results of the regression analysis are depicted graphically in Fig. 6c and d. The mean hourly UHII was found to have a strong positive correlation with both ΔDI ($r_{obs} = 0.7$) and ΔAWBGT ($r_{obs} = 0.6$). A two-tailed $t$-test confirms this strong relation with $p < 0.001$ at both cases. This indicates that the city's heat island may have a strong impact on discomfort and heat stress conditions. In particular, higher UHII values appear to deteriorate thermal comfort and heat stress conditions, resulting to increased DI and AWBGT values.

However, both UHII and ΔDI or ΔAWBGT share a common variable, namely air temperature, and as such there is in principle the possibility that the observed relationship between these quantities is partially spurious. In order to test this possibility and to confirm or revise the previously reported findings, the magnitude of self-correlation between UHII, and ΔDI and ΔAWBGT was defined applying the methodology of Klipp and Mahrt (2004). In brief, random datasets containing uncorrelated values for air temperature, relative humidity and water vapor pressure were created using the original hourly observations as a pool of values to draw from at random. Using the random data, new values for the UHII, and the DI and AWBGT differences were computed and the correlation coefficient between them was calculated. This process was repeated many times and several correlation coefficients were obtained. Since the randomized data no longer retained any physical connections between the aforementioned basic variables, the estimated average correlation coefficient is considered to be a measure of the self-correlation due to the presence of the common variable (i.e. air temperature).

By applying the above described methodology, it was found that the randomized UHII data yield a self-correlation coefficient of 0.5 ($r_{rand} = 0.5$) with ΔDI and 0.3 ($r_{rand} = 0.3$) with ΔAWBGT. Assuming that the square of the correlation coefficient ($r^2$) is a measure of the percent of the variance in the data that can be explained by a linear model (Klipp and Mahrt, 2004), it is evident that in the present study an important part of the variance of ΔDI and ΔAWBGT explained by UHII is associated with self-correlation. Indeed, the variance explained by self-correlation is about 50% of the observed variance of ΔDI ($r_{obs}^2 = 0.49$, $r_{rand}^2 = 0.25$) and 25% of the observed variance of ΔAWBGT ($r_{obs}^2 = 0.36$, $r_{rand}^2 = 0.09$). That is, one half and one quarter of the observed variance of ΔDI and ΔAWBGT, respectively, explained by UHII is attributed to self-correlation.

Taking into account the above presented results, it becomes clear that a more intense UHI does not always result to increased DI or AWBGT values in the metropolitan area of Thessaloniki compared to the surrounding area represented by station 7. However, it can be deduced that, on average, higher UHII values result to greater DI and AWBGT values in the city than in the less urbanized surroundings on 50% and 75% of the cases.

## 5. Conclusions

The aim of this study is to provide an analysis of the UHI in a coastal Mediterranean city; Thessaloniki, Greece. The study is based on time series analysis of air temperature and relative humidity measurements that were carried out at seven sites in the greater Thessaloniki area. The monthly and hourly variation of air temperature in six urban and one semi-rural station were determined, showing that the urban zone of the city is generally warmer compared to its surroundings. The analysis of the air temperature data revealed that the urban areas of study store heat more effectively, resulting to elevated temperatures, especially during nighttime and early morning hours.

The UHII was selected as an index for analyzing the impact of the urban environment on air temperature. The daily mean, maximum and minimum values of the heat island intensity were determined for every season of the year. It was deduced that a clear seasonal variation cannot be drawn based on these season-averaged values. However, the conducted analysis provided indications for a more pronounced UHI during the warmer period of the year than during the colder months. It was also found that the UHII shows a small variability in the summer season (UHII~2–3 °C), whereas during winter months a greater variability occurs. Additionally, it was found that the city of Thessaloniki exhibits the opposite to UHI phenomenon; the UCI. The detailed analysis of the hourly UHII data revealed that the heat island intensity decreases following sunrise, reaching its minimum at early afternoon hours and increasing again as daytime ends.

Furthermore, the impact of wind conditions on the intensity of the UHI effect was analyzed. It was found that the UHI is more pronounced when wind is weak, whereas the UHII is significantly reduced when wind speed exceeds 4 m/s. The possible impact of the coastal environment on the UHI was also examined and discussed, using air temperature and relative humidity measurements to derive water vapor pressure. As observed, the city of Thessaloniki exhibits the

so-called UME phenomenon that is characterized by higher moisture availability in the urban areas than in the semi-rural site. The conducted analysis revealed that the nocturnal UHI precedes the UME, whereas during the day the two effects are rather negatively correlated.

Finally, the present study examined the potential impact of the UHI on human thermal comfort. Considering only the observations that were made during the summer months, hourly values of Thom's DI and AWBGT were calculated and analyzed in detail. It was shown that August exhibits the highest DI and AWBGT values in all examined sites, while the diurnal variation of both indices follows closely the respective variation of air temperature. It was noted that the feeling of discomfort and heat stress danger are maximum at early afternoon hours, decreasing as daytime ends. More interestingly, it was observed that the center of the city maintains high DI and AWBGT values (greater than 24 °C and 27.7 °C, respectively) for a prolonged time period of 12 and 9 h, respectively. This indicates that the population of this area is subject to discomfort and heat stress conditions during most hours of the day. Furthermore, the correlation between the UHII and the two indices was examined and discussed. It was observed that the UHII has a strong positive correlation with both DI and AWBGT differences; the UHI results to deterioration of thermal comfort and heat stress conditions. However, it was also shown that a significant part of this relationship is attributed to self-correlation between UHII, and ΔDI and ΔAWBGT.

Therefore, it was concluded that the heat island of Thessaloniki has a negative impact on the experienced thermal comfort and heat stress conditions on most occasions but not always. For instance, a 1.5 °C increase in the intensity of the heat island would cause an average 1 °C increase in DI and 1.4 °C in AWBGT of the urban area on approximately 50% and 75% of the cases, respectively.

## Abbreviations

| | |
|---|---|
| ΔAWBGT | Approximated wet-bulb globe temperature difference |
| ΔDI | Discomfort index difference |
| Δe | Water vapor pressure difference |
| ΔRH | Relative humidity difference |
| AWBGT | Approximated wet-bulb globe temperature |
| DI | Discomfort index |
| DJF | December January February |
| JJA | June July August |
| LT | Local time |
| MAM | March April May |
| RH | Relative humidity |
| SON | September October November |
| UBL | Urban boundary layer |
| UCI | Urban cool island |
| UCL | Urban canopy layer |
| UHI | Urban heat island |
| UHII | Urban heat island intensity |
| $UHII_{min}$ | Daily minimum urban heat island intensity |
| $UHII_{max}$ | Daily maximum urban heat island intensity |
| $UHII_{mean}$ | Daily mean urban heat island intensity |
| UME | Urban moisture excess |

## References

Ackerman, B., 1971. Moisture content of city and country air. Pre-prints Conf. on Air Pollution Meteorology, Raleigh, Am. Meteorol. Soc. 154–158 pp.

Ackerman, B., 1987. Climatology of Chicago area urban–rural differences in humidity. J. Clim. Appl. Meteorol. 26, 427–430.

Alonso, M.S., Labajo, J.L., Fidalgo, M.R., 2003. Characteristics of the urban heat island in the city of Salamanca, Spain. Atmosfera 16 (3), 137–148.

Angouridakis, V.E., Makrogiannis, T.J., 1982. The discomfort index in Thessaloniki, Greece. Int. J. Biometeorol. 26, 53–59.

Arnfield, A.J., 2003. Two decades of urban climate research: a review of turbulence, exchanges of energy and water, and the urban heat island. Int. J. Climatol. 23, 1–26.

Bassara, J.P., Hall Jr., P.K., Schroeder, A.J., Illston, B.G., Nemunaities, K.L., 2008. Diurnal cycle of the Oklahoma City urban heat island. J. Geophys. Res. 113, 1–16.

Buechley, R.W., Van Bruggen, J., Truppi, L.E., 1972. Heat islands equal death islands? Environ. Res. 5, 85–92.

Chandler, T.J., 1967. Absolute and relative humidities in towns. Bull. Am. Meteorol. Soc. 48, 394–399.

Chang, C.R., Li, M.H., Chang, S.D., 2007. A preliminary study of the local cool-island intensity of Taipei city parks. Landsc. Urban Plann. 80, 386–395.

Christen, A., Vogt, R., 2004. Energy and radiation balance of a central European city. Int. J. Climatol. 24, 1395–1421.

Clarke, J.F., 1972. Some effects of the urban structure on heat mortality. Environ. Res. 5, 93–104.

Conti, S., Meli, P., Mineli, G., Solimini, R., Toccaceli, V., Vichi, M., Beltrano, C., Perini, L., 2005. Epidemiologic study of mortality during the summer 2003 heat wave in Italy. Environ. Res. 98, 390–399.

Coutts, A.M., Beringer, J., Tapper, N.J., 2003. Impact of increasing urban density on local climate: spatial and temporal variations in the surface energy balance in Melbourne, Australia. J. Appl. Meteorol. 46, 477–493.

Figuerola, P.I., Mazzeo, N.A., 1999. Urban–rural temperature differences in Buenos Aires. Int. J. Climatol. 18, 1709–1723.

Fortuniak, K., Klysik, K., Wibig, J., 2006. Urban–rural contrasts of meteorological parameters in Lodz. Theor. Appl. Climatol. 84, 91–101.

Giannaros, T.M., Melas, D., Kontogianni, P., 2010. An observational study of the urban heat island in the greater Thessaloniki area: preliminary results and development of a forecasting service. AIP Conf. Proc. 1203, 991–996.

Giannopoulou, K., Livada, I., Santamouris, M., Saliari, M., Assimakopoulos, M., Caouris, Y.G., 2011. On the characteristics of the summer urban heat island in Athens, Greece. Sustain. Cities Dev. 1, 16–28.

Giles, B.D., Flocas, A.A., 1990. Diurnal rainfall variations in Thessaloniki, Greece. Theor. Appl. Climatol. 41, 221–225.

Giridharan, R., Ganesan, S., Lau, S.S.Y., 2004. Daytime urban heat island effect in high-rise and high-density residential developments in Hong Kong. Energ. Build. 36, 525–534.

Grimmond, C.S.B., Oke, T.R., 1995. Comparison of heat fluxes from summertime observations in the suburbs of four North American cities. J. Appl. Meteorol. 34, 873–889.

Grimmond, C.S.B., Oke, T.R., 1999. Aerodynamic properties of urban areas derived from analysis of surface form. J. Appl. Meteorol. 38, 1262–1292.

Grimmond, C.S.B., Souch, C., Hubble, M.D., 1996. Influence of tree cover on summertime surface energy balance fluxes, San Gabriel Valley, Los Angeles. Clim. Res. 6, 45–57.

Hacker, J.N., Belcher, S.E., Connell, R.K., 2005. Beating the Heat: Keeping UK Buildings Cool in a Warming Climate. Climate Impacts Programme, Oxford, United Kingdom.

Hage, K.D., 1975. Urban–rural humidity differences. J. Appl. Meteorol. 14, 1277–1283.

Hellenic National Meteorological Service http://www.hnms.gr, last accessed on 1 August 2011.

Holmer, B., Eliasson, I., 1999. Urban–rural vapour pressure differences and their role in the development of urban heat islands. Int. J. Climatol. 19, 989–1009.

Howard, L., 1883. The Climate of London, vols. I–III. Harvey and Dorton, London.

Hung, T., Uchihama, D., Ochi, S., Yasuoka, Y., 2006. Assessment with satellite data of the urban heat island effects in Asian mega cities. Int. J. Appl. Earth Obs. 8 (1), 34–48.

Jauregui, E., 1997. Heat island development in Mexico City. Atmos. Environ. 31, 3821–3831.

Jauregui, E., Tejeda, A., 1997. Urban–rural humidity contrasts in Mexico City. Int. J. Climatol. 17, 187–196.

Jones, T.S., Liang, A.P., Kilboume, E.M., et al., 1982. Morbidity and mortality associated with the July 1980 heat wave in St. Louis and Kansas City Mo. J. Am. Med. Assoc. 247, 3327–3331.

Kantzioura, A., Kosmopoulos, P., Zoras, S., 2012. Urban surface temperature and microclimate measurements in Thessaloniki. Energ. Build. 44, 63–72.

Kassomenos, P.A., Katsoulis, B.D., 2006. Mesoscale and macroscale aspects of the morning urban heat island around Athens, Greece. Meteorol. Atmos. Phys. 94, 209–218.

Katsoulis, B.D., 1987. Indications of change of climate from the analysis of air temperature time series in Athens, Greece. Clim. Chang. 10, 67–79.

Katsoulis, B.D., Theoharatos, G.A., 1995. Indications of the urban heat island in Athens, Greece. J. Clim. Appl. Meteorol. 24, 1296–1301.

Kidder, S.Q., Essenwanger, O.M., 1995. The effects of clouds and wind on the difference in nocturnal cooling rates between urban and rural areas. J. Appl. Meteorol. 34, 2440–2448.

Kim, Y., Baik, J., 2002. Maximum urban heat island intensity in Seoul. J. Appl. Meteorol. 41, 651–659.

Kim, Y., Baik, J., 2004. Daily maximum urban heat island intensity in large cities of Korea. Theor. Appl. Climatol. 79, 151–164.

Kim, Y., Baik, J., 2005. Spatial and temporal structure of the urban heat island in Seoul. J. Appl. Meteorol. 44, 591–605.

Klipp, C.L., Mahrt, L., 2004. Flux-gradient relationship, self-correlation and intermittency in the stable boundary layer. Q. J. R. Meteorol. Soc. 130, 2087–2103.

Klyzik, K., Fortuniak, K., 1999. Temporal and spatial characteristics of the urban heat island of Lódz, Poland. Atmos. Environ. 33, 3885–3895.

Kolokotsa, D., Psomas, A., Karapidakis, E., 2009. Urban heat island in Southern Europe: the case study of Hania, Crete. Sol. Energy 83, 1871–1883.

Konopacki, S., Akbari, H., 2002. Energy savings for heat island reduction strategies in Chicago and Houston (including updates for Baton Rouge, Sacramento, and Salt Lake City). Draft Final Report, LBNL-49638. University of California, Berkeley.

Kuttler, W., Weber, S., Schonnefeld, J., Hesselschwerdt, A., 2007. Urban/rural atmospheric water vapour differences and urban moisture excess in Krefeld, Germany. Int. J. Climatol. 25, 2005–2015.

Lee, D.O., 1991. Urban–rural humidity differences in London. Int. J. Climatol. 11, 577–582.

Lee, S.H., Baik, J.J., 2010. Statistical and dynamical characteristics of the urban heat island intensity in Seoul. Theor. Appl. Climatol. 100, 227–237.

Livada, I., Santamouris, M., Niachou, K., Papanikolaou, M., Michalakakou, G., 2002. Determination of places in the great Athens area where the heat island effect is observed. Theor. Appl. Cimatol. 71, 219–230.

Maheras, P., Patrikas, I., Karacostas, Th., Anagnostopoulou, Chr, 2000. Automatic classification of circulation types in Greece: methodology, description, frequency, variability and trend analysis. Theor. Appl. Climatol. 67, 205–223.

Matzarakis, A., De Rocco, M., Najjar, G., 2009. Thermal bioclimate in Strasbourg — the 2003 heat wave. Theor. Appl. Climatol. 98, 209–220.

Mavrogianni, A., Davies, M., Batty, M., et al., 2011. The comfort, energy and health implications of London's urban heat island. Build. Serv. Eng. Res. Technol. 32 (1), 35–52.

Melas, D., Ziomas, I.C., Zerefos, C.S., 1994. A numerical study of dispersion in a coastal urban area. Part A. Air flow. Fresenius Environ. Bull. 3, 306–311.

Memon, R.A., Leung, D.Y.C., Liu, C.-H., 2009. An investigation of urban heat island intensity (UHII) as an indicator of urban heating. Atmos. Res. 94, 491–500.

Miao, S., Chen, F., LeMone, A.M., Tewari, M., Li, Q., Wang, Y., 2009. An observational and modelling study of characteristics of urban heat island and boundary layer structures in Beijing. J. Appl. Meteorol. Clim. 48, 484–501.

Montavez, J.P., Rodriguez, A., Jimenez, J.I., 2000. A study of the urban heat island of Granada. Int. J. Climatol. 20, 899–911.

Morris, C.J.C., Simmonds, I., 2000. Associations between varying magnitudes of the urban heat island and the synoptic climatology in Melbourne, Australia. Int. J. Climatol. 20, 1931–1954.

Morris, C.J.C., Simmonds, I., Plummer, N., 2001. Quantification of the influences of wind and cloud on the nocturnal urban heat island of a large city. J. Appl. Meteorol. 40, 169–182.

Moussiopoulos, N., Papalexiou, S., Sahm, P., 2006. Wind flow and photochemical air pollution in Thessaloniki, Greece. Part I: Simulations with the European Zooming Model. Environ. Model. Sofw. 12, 1752–1758.

Oke, T.R., 1982. The energetic basis of the urban heat island. Q. J. Roy. Meteor. Soc. 108, 1–24.

Oke, T.R., 1988. The urban energy balance. Phys. Geogr. 12, 1–24.

Oke, T.R., 1995. The heat island characteristics of the urban boundary layer: characteristics, causes and effects. In: Cermak, J.E., Davenport, A.G., Plate, E.J., Viegas, D.X. (Eds.), Wind Climate in Cities, pp. 81–102.

Papanastasiou, D.K., Kittas, C., 2011. Maximum urban heat island intensity in a medium-sized coastal Mediterranean city. Theor. Appl. Climatol. 107, 407–416.

Papanastasiou, D.K., Melas, D., Bartzanas, T., Kittas, C., 2010. Temperature, comfort and pollution levels during heat waves and the role of sea breeze. Int. J. Biometeorol. 54, 307–317.

Papanikolaou, N., Livada, I., Santamouris, M., Niachou, K., 2008. The influence of wind speed on heat island phenomenon in Athens, Greece. Int. J. Vent. 6, 337–348.

Philandras, C.M., Metaxas, D.A., Nastos, P.Th., 1999. Climate variability and urbanization in Athens. Theor. Appl. Climatol. 63, 65–72.

Pigeon, G., Legain, D., Durand, P., Masson, V., 2007. Anthropogenic heat release in an old European agglomeration (Toulouse, France). Int. J. Climatol. 27, 1969–1981.

Pinho, O.S., Manso Orgaz, M.D., 2002. The urban heat island in a small city in coastal Portugal. Int. J. Biometeorol. 44, 198–203.

Pongracz, R., Bartholy, J., Deszo, Z., 2006. Remotely sensed thermal information applied to urban climate analysis. Adv. Space Res. 37 (12), 2191–2196.

Poupkou, A., Nastos, P., Melas, D., Zerefos, C., 2011. Climatology of discomfort index and air quality index in a large urban mediterranean agglomeration. Water Air Soil Pollut. 222, 163–183.

Rosenfeld, A.H., Akbari, H., Romn, J.J., Pomerantz, M., 1998. Cool communities: strategies for heat island mitigation and smog reduction. Energ. Build. 28, 51–62.

Sahsamanoglou, C.S., 1976. The sea breeze in Thessaloniki. Bull. Hell. Meteorol. Soc. 1, 19–33 (in Greek).

Santamouris, M., 2007. Heat island research in Europe: the state of the art. Adv. Build. Energy Res. 1, 123–150.

Santamouris, M., Papanikolaou, N., Livada, I., Koronakis, I., Georgakis, C., Assimakopoulos, D.N., 2001. On the impact of urban climate to the energy consumption of buildings. Sol. Energy 70 (3), 201–216.

Shigeta, Y., Ohashi, Y., Tsukamoto, O., 2009. Urban cool island in daytime — analysis by using thermal image and air temperature measurements. The Seventh International Conference on Urban Climate, 29 June – 3 July 2009, Yokohama, Japan.

Smoyer, K.E., 1998. Putting risk in its place: methodological considerations for investigating extreme event health risk. Soc. Sci. Med. 47, 1809–1824.

Steeneveld, G.J., Koopmans, S., Heusinkveld, B.G., van Howe, L.W.A., Holtslag, A.A.M., 2011. Quantifying urban heat island effects and human comfort for cities of variable size and urban morphology in the Netherlands. J. Geophys. Res. 117, D20129.

Stewart, I.D., 2011. A systematic review and scientific critique of methodology in modern urban heat island literature. Int. J. Climatol. 31, 200–217.

Stewart, I.D., Oke, T.R., 2009a. Conference notebook — a new classification system for urban climate sites. Bull. Am. Meteorol. Soc. 90, 922–923.

Stewart, I.D., Oke, T.R., 2009b. Classifying urban climate field sites by "local climate zones": the case of Nagano, Japan. Preprints Seventh International Conference on Urban Climate, June 29–July 3 2009, Yokohama, Japan.

Stewart, I.D., Oke, T.R., 2010. Thermal differentiation of local climate zones using temperature observations from urban and rural field sites. Ninth Symposium on the Urban Environment, 2–6 August 2010, Keystone, Colorado, United States.

Streutker, D.R., 2003. Satellite-measured growth of the urban heat island of Houston, Texas. Remote. Sens. Environ. 85, 282–289.

Thom, E.C., 1959. The discomfort index. Weatherwise 12, 57–60.

Voogt, J.A., Oke, T.R., 2003. Thermal remote sensing of urban climates. Remote. Sens. Environ. 86, 370–384.

Weber, S., Kuttler, W., 2005. Surface energy-balance characteristics of a heterogeneous urban ballast facet. Clim. Res. 28, 257–266.

World Meteorological Organization, 2000. General meteorological standards and recommended practices. Appendix A, WMO Technical Regulations, WMO-No. 49.

World Urbanization Prospects, 2007. The 2007 Revision Population Database. http://esa.un.org/unup/, last accessed 1 August 2011.

**Mr. Theodore M. Giannaros** was born in 1982 in Thessaloniki, Greece. He graduated from the School of Physics of the Aristotle University of Thessaloniki (AUTH) in 2005 and received his M.Sc. in Environmental Physics from AUTH in 2007. He is currently carrying out his Ph.D. at the Laboratory of Atmospheric Physics (LAP) of AUTH. He is actively involved in scientific research for more than 4 years. His main research interests and expertise include the implementation of numerical modeling and data assimilation techniques for studying the urban heat island effect and thermal comfort in urban areas.

**Dr. Dimitrios Melas** was born in 1958 in Thessaloniki, Greece. He graduated from the School of Physics of the University of Ioannina in 1982 and received his Ph.D. in Meteorology from the Institute of Meteorology of the University of Upssala, Sweden, in 1990. He is currently Associate Professor and a member of the Laboratory of Atmospheric Physics (LAP) of the Aristotle University of Thessaloniki (AUTH). He is involved in scientific research for more than 25 years. His research interests are focused on atmospheric boundary layer research, air quality modeling and monitoring, meteorology and environmental physics.